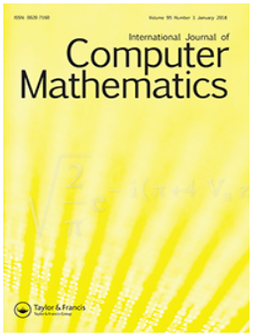

International Journal of Computer Mathematics

ISSN: 0020-7160 (Print) 1029-0265 (Online) Journal homepage: http://www.tandfonline.com/loi/gcom20

An adaptive FEM with ITP approach for steady Schrödinger equation

Yang Kuang & Guanghui Hu

To cite this article: Yang Kuang & Guanghui Hu (2018) An adaptive FEM with ITP approach for steady Schrödinger equation, International Journal of Computer Mathematics, 95:1, 187-201, DOI: 10.1080/00207160.2017.1366463

To link to this article: https://doi.org/10.1080/00207160.2017.1366463

Accepted author version posted online: 10 Aug 2017.
Published online: 24 Aug 2017.

INTERNATIONAL JOURNAL OF COMPUTER MATHEMATICS, 2018
VOL. 95, NO. 1, 187–201
https://doi.org/10.1080/00207160.2017.1366463

Taylor & Francis
Taylor & Francis Group

ARTICLE

An adaptive FEM with ITP approach for steady Schrödinger equation

Yang Kuang[a] and Guanghui Hu[a,b]

[a]Department of Mathematics, Faculty of Science and Technology, University of Macau, Macao SAR, China; [b]UM Zhuhai Research Institute, Guangdong, China

ABSTRACT

In this paper, an adaptive numerical method is proposed for solving a 2D Schrödinger equation with an imaginary time propagation approach. The differential equation is first transferred via a Wick rotation to a real time-dependent equation, whose solution corresponds to the ground state of a given system when time approaches infinity. The temporal equation is then discretized spatially via a finite element method, and temporally utilizing a Crank–Nicolson scheme. A moving mesh strategy based on harmonic maps is considered to eliminate possible singular behaviour of the solution. Several linear and nonlinear examples are tested by using our method. The experiments demonstrate clearly that our method provides an effective way to locate the ground state of the equations through underlying eigenvalue problems.

ARTICLE HISTORY
Received 20 February 2017
Revised 12 June 2017
Accepted 26 June 2017

KEYWORDS
Schrödinger equation; imaginary time propagation; moving mesh method; finite element method; ground state

2010 AMS SUBJECT CLASSIFICATIONS
65N30; 35Q40

1. Introduction

The ground state of a given quantum system describes its lowest energy state. The study of the ground state plays an important role in a variety of areas such as molecular geometry optimization, photon-absorption spectra of atoms and molecules, linear response theory in the molecular dynamics. One popular method to calculate the ground states of given quantum systems is to solve eigenvalue problems derived from the governing equations such as the Schrödinger equation and the Kohn–Sham equation [11] for the electronic structure calculations, and the Gross–Pitaevskii equation [13,23] for the quantum system of identical bosons. Specifically, the form of the time-independent Schrödinger equation is written as

$$H\psi = E\psi, \tag{1}$$

where H is the Hamiltonian, and E and ψ represent the eigenenergy and wavefunction, respectively. By discretizing the above equation with certain method, the ground state of the given system is obtained by solving the following generalized eigenvalue problem

$$A\psi_h = \varepsilon_h B\psi_h, \tag{2}$$

where (ε_h, ψ_h) denotes the approximate eigenpair, and A and B are two discretization method dependent matrices.

There are many mature methods for the discretization of (1), for example, the plan-wave expansion method [14], the finite difference method [10], the finite element method [2,22,26], the wavelet

CONTACT Guanghui Hu garyhu@umac.mo

method [27], the discontinuous Galerkin method [19], etc. For a many particle system, the Hamiltonian H would depend on the wavefunction ψ, which makes the equation nonlinear. Hence, the generalized eigenvalue problem (2) is also a nonlinear one. In the numerical simulation, the linearization method is necessary in solving (2), and the most popular one is the self-consistent field (SCF) iteration. SCF iteration is quite simple, and can be described as follows. Suppose that the eigenpair $(\varepsilon^{(k)}, \psi^{(k)})$ at the kth iteration step is known, then the new eigenpair $(\varepsilon^{(k+1)}, \psi^{(k+1)})$ is obtained by solving the linear generalized eigenvalue problem $A(\psi^{(k)})\psi^{(k+1)} = \varepsilon^{(k+1)}\psi^{(k+1)}$. The iteration is stopped when $||\psi^{(k+1)} - \psi^{(k)}||$ is less than a given tolerance. To date, although there are several techniques such as mixing scheme for improving the convergence of the iteration, the theoretically guaranteed convergent method is still desired. In the practical simulations, the convergence of the SCF iteration sometimes is uncertain, especially when the given electronic structure is large scale and complicated. The issue motivates the study on the alternative methods, instead of solving the nonlinear eigenvalue problem, for the ground state calculation.

A widely-used method is the imaginary time propagation (ITP) method [4,5,15,24,28], in which the complex-valued time-dependent Schrödinger equation is transferred to a real-valued time-dependent problem by introducing the imaginary time. The ground state of the given system can be obtained by propagating the real-valued system till the imaginary time approaches infinity. With this method, solving nonlinear eigenvalue problem is avoided, and the derived real-valued time-dependent equation can be handled well with the classical methods. In the design of the algorithm, the following two features are desired. First, the time propagation scheme should be stable and efficient. Since the system needs to be propagated in a sufficiently long time to get a good approximation for the ground state, a large time step in the simulation is desired to reduce the total propagation steps. Also, the calculation in each time propagation step should also be efficient. Second, the algorithm should be flexible enough to handle the computational domain with complicated geometry and various boundary conditions.

To satisfy the above two requirements, the numerical method should be designed carefully. For the temporal discretization, several classical schemes are available such as Euler schemes, Crank–Nicolson scheme, Runge–Kutta schemes. Among these schemes, the implicit ones are the first choice since their advantage on the stability. To match the numerical accuracy from the spatial discretization, that is, linear finite element discretization, the second-order Crank–Nicolson scheme will be used to serve the temporal discretization of the governing equation. For the spatial discretization, the following observations motivate us to use the finite element method. First of all, the finite element method can handle the unstructured mesh in a natural way. With appropriate basis functions, the finite element space can be built on both triangle and rectangle meshes, or even on the mesh with mixed elements. It also means that complex domain can be handled flexibly, which is important for the practical simulations. Secondly, unlike the spectral method, the basis function for the finite element method is local, which would result in a sparse system. An efficient solver such as algebraic multigrid method together with a quality data structure for saving the sparse matrix would make the solve of the linear system very efficient. Finally, to further improve the simulation efficiency, the adaptive method based on the finite element framework can be used for more efficient spatial discretization. This is particularly useful when there is singularity in the numerical solution. In the market, a competitive candidate for solving the derived temporal equation is the operator splitting scheme [12,20,21]. For example, in [25], it is proved that Strang splitting scheme is unconditionally stable for linear problem with monotone operator. A typical scene for operator splitting scheme is that the time propagator is expressed by the matrix exponential, then fast Fourier transform (FFT) provides fast calculation. However, the use of FFT introduces the dependence of the scheme on the regular domain and mesh grids, which bring limitation of the scheme on the practical applications. It is worth mentioning that the idea of operator splitting can still show its power in the proposed method by separating linear and nonlinear part in the Hamiltonian operator and propagating them in order. With this strategy, the simulation could be further accelerated. The study on this issue will be reported in the forthcoming paper.

In this paper, a framework of adaptive finite element solutions for ground state calculation of a given quantum system is proposed. The complex-valued temporal Schrödinger equation is transferred to a real-valued temporal equation by Wick rotation first. Then the equation is discretized temporally by Crank–Nicolson method, and spatially by linear finite element method. The moving mesh method based on the harmonic maps [8,16] is introduced to improve the simulation efficiency. The issues on the mesh movement and solution update are discussed in detail. Particularly, the design of the monitor function, which is crucial for controlling the mesh quality, is studied in depth. The effectiveness of the proposed method is demonstrated by a variety of examples including linear and nonlinear problems.

This paper is organized as follows. In Section 2, the numerical issues including the ITP technique and the numerical discretization for the Schrödinger equation are introduced. The mesh redistribution part will be discussed in detail in Section 3. Then three numerical experiments are demonstrated in Section 4. Finally, the conclusion is given.

2. Numerical discretization

In this section, we will propose a numerical method by propagating the Schrödinger equation in imaginary time via adaptive finite element discretization in space and Crank–Nicolson discretization in time to solve the stationary Schrödinger equation.

2.1. Imaginary time propagation

ITP is often used as a solver for the eigenvalue problems such as the time-independent Schrödinger equation (1). The basic idea of the ITP method origins from the fact that the set of eigenstates $\{\phi_j\}$ of the Hamiltonian H forms a real orthonormal basis on its domain. To illustrate the ITP method, we consider the ground state of a quantum system which can be modelled by a stationary Schrödinger equation as shown in Equation (1). Actually, this time-independent Schrödinger equation originates from the time-dependent Schrödinger equation

$$\mathrm{i}\frac{\partial \psi(\boldsymbol{r},t)}{\partial t} = H\psi(\boldsymbol{r},t), \quad \psi(\boldsymbol{r},0) = \psi_0(\boldsymbol{r}). \tag{3}$$

Here $\psi_0(\boldsymbol{r})$ is the initial condition and H can be written as

$$H = -\tfrac{1}{2}\nabla^2 + v(\boldsymbol{r},t),$$

where $v(\boldsymbol{r},t)$ stands for the potential field due to the nuclei and electrons. A Wick rotation of the time coordinate, $t = -\mathrm{i}\tau$, transforms (3) into the following type equation:

$$-\frac{\partial \psi(\boldsymbol{r},\tau)}{\partial \tau} = H\psi(\boldsymbol{r},\tau), \quad \psi(\boldsymbol{r},0) = \psi_0(\boldsymbol{r}), \tag{4}$$

with the formal solution $\psi(\boldsymbol{r},\tau) = \mathrm{e}^{-\tau H}\psi_0\boldsymbol{r}$. Assume $\{E_i\}$ is the set of the eigenvalues of the Hamiltonian operator H corresponding to the eigenstates $\{\phi_i\}$ with an increasing order, that is, $E_0 \le E_1 \le \cdots \le E_i \le \cdots$. After expanding the initial condition ψ_0 in the basis of eigenstates $\{\phi_j\}$,

$$\psi_0(\boldsymbol{r}) = \sum_i c_i\phi_i(\boldsymbol{r}), \quad c_i = \langle \phi_i(\boldsymbol{r})|\psi_0(\boldsymbol{r})\rangle,$$

the time evolution of (4) is given by

$$\psi(\boldsymbol{r},\tau) = \mathrm{e}^{-\tau H}\psi_0(\boldsymbol{r}) = \sum_i \mathrm{e}^{-\tau E_i}c_i\phi_i(\boldsymbol{r}) = \mathrm{e}^{-\tau E_0}\sum_i \mathrm{e}^{-\tau(E_i-E_0)}c_i\phi_i(\boldsymbol{r}). \tag{5}$$

Asymptotically, if the initial state ψ_0 is not orthogonal to the ground state ϕ_0, then after a sufficiently long time propagation, we get $\psi(\boldsymbol{r},\tau) \to \mathrm{e}^{-\tau E_0}c_0\phi_0$ since the other exponentials decay more

rapidly. The wavefunction for the ground state then can be obtained by normalizing $\psi(\boldsymbol{r},\tau)$. To achieve the excited states, we can propagate several different initial states simultaneously in time with an orthogonalization process after each step.

2.2. Temporal discretization

To approximate the time evolution (5), that is, the exponential $\mathrm{e}^{-\tau H}$, one can use the operator splitting methods which evaluate compositions of the operators $\mathrm{e}^{-\tau V}$ and $\mathrm{e}^{-\tau T}$ at different times, where $T = -\frac{1}{2}\nabla^2$. For instance, the well-known Strang splitting

$$\Psi_h = \mathrm{e}^{-(h/2)V}\,\mathrm{e}^{-hT}\,\mathrm{e}^{-(h/2)V} \tag{6}$$

gives a second-order approximation with $h = \Delta\tau$. Propagation of operator $\mathrm{e}^{-\frac{h}{2}V}$ in Equation (6) is evaluated in the coordinate spaces, while the other component operator e^{-hT} is evaluated in the momentum spaces. To communicate information between coordinate space and momentum space, the FFT technique is thus carried out. However, taking the requirements of FFT into account, difficulties will appear if we consider the general problems with the non-uniform mesh on the computational domain or with the non-periodic boundary condition. We thus return back to consider the equation (4) and solve it directly.

As the Crank–Nicolson method allows a relatively large time step and the moving mesh method provides a desired mesh for handling the singularities, we discretize (4) in time by Crank–Nicolson method and in space by finite element method. It is noteworthy that due to the functional dependence on the density, problem (4) becomes nonlinear, which will be handled by a prediction–correction procedure in this paper.

For simplicity, we now only consider the time-dependent Schrödinger equation corresponding to the ground state of which the initial state can be arbitrary as lone as it is not orthogonal to the ground state. And the excited states can be treated basically in the same way only with the different initial conditions and requiring the orthogonality to other states.

As the Crank–Nicolson method is numerically stable and is a second-order method in time, we apply this method to propagate the system in the imaginary time.

Let the superscript (n) denote the representation of the corresponded term at time $\tau = n\Delta\tau$, where $\Delta\tau$ is the time step. Suppose we have obtained the wavefunction at time $n\Delta\tau$, to achieve the ground state ϕ_0 associated with the lowest eigenvalue E_0 of (4), we solve the time evolution problem by applying the Crank–Nicolson method for temporal discretization on (4)

$$-\frac{\psi^{(n+1)} - \psi^{(n)}}{\Delta\tau} = \frac{1}{2}(H^{(n+1)}\psi^{(n+1)} + H^{(n)}\psi^{(n)}), \quad \psi^{(0)} = \psi_0. \tag{7}$$

Rearranging the terms we have

$$\left(H^{(n+1)} + \frac{2}{\Delta\tau}\right)\psi^{(n+1)} = \left(-H^{(n)} + \frac{2}{\Delta\tau}\right)\psi^{(n)}, \tag{8}$$

with $H^{(n)} = -\nabla^2/2 + v^{(n)}$.

2.3. Finite element method for spatial discretization

In finite element method the wave function $\psi(\mathbf{r})$ is expanded as a sum of the piecewise-polynomial basis functions $\{\varphi_i\}$ on a set of real space interpolation nodes with a set of coefficients $\{\psi_i\}$,

$$\psi(\mathbf{r}) = \sum_{i}^{N_{\text{basis}}} \psi_i\varphi_i, \tag{9}$$

where N_{basis} stands for the dimension of space V_h spanned by the basis functions, and ψ_i is the ith basis function which is typically chosen in such a way that ψ_i is 1 on ith finite element interpolation node while 0 on all other nodes. As a result, the ith coefficient of the wave function ψ_i is actually the value of the wave function itself on the corresponding nodes.

To find an approximate solution, we discretize the equation within the subspace V_h. In this way, solving Equation (8) is reduced to solve the following system

$$A\psi^{(n+1)} = B\psi^{(n)}. \tag{10}$$

Here A and B are two matrices with the entries

$$A_{i,j} = \frac{1}{2}\int_\Omega (\nabla\varphi_i \cdot \nabla\varphi_j)\,\mathrm{d}\mathbf{r} + \int_\Omega v^{(n+1)}\varphi_i\varphi_j\,\mathrm{d}\mathbf{r} + \frac{2}{\Delta\tau}\int_\Omega \varphi_i\varphi_j\,\mathrm{d}\mathbf{r}, \tag{11}$$

$$B_{i,j} = -\frac{1}{2}\int_\Omega (\nabla\varphi_i \cdot \nabla\varphi_j)\,\mathrm{d}\mathbf{r} - \int_\Omega v^{(n)}\varphi_i\varphi_j\,\mathrm{d}\mathbf{r} + \frac{2}{\Delta\tau}\int_\Omega \varphi_i\varphi_j\,\mathrm{d}\mathbf{r}. \tag{12}$$

Therefore, if $A_{i,j}$ and $B_{i,j}$ are clear, we can obtain $\psi^{(n+1)}$ from the system (10), and we can attain the excited states in this same way with the same $A_{i,j}$ and $B_{i,j}$. Since all the states are required to be orthonormal, we need to orthogonalize these states after each step. Here we use the Gram-Schmidt method to orthogonalize these states.

While back to the system (10), note that the potential term $v^{(n+1)}$ might rely on the $\psi^{(n+1)}$, for example, the coupled Gross–Pitaevskii system, which leads (10) to be a nonlinear system. Therefore, the potential $v^{(n+1)}$ must be obtained by iterative methods. That is, the wave function $\{\psi^{(n+1)}\}$ is solved from Equation (10), and then the potential $v^{(n+1)}(\mathbf{r})$ is updated with respect to the new wavefunction. In this way we can obtain the new wavefunction $\{\psi^{(n+1)}\}$ and then the new $v^{(n+1)}(\mathbf{r})$ and so forth. To end up the iterations, the following criterion is used

$$\|v_{k+1}^{(n+1)} - v_k^{(n+1)}\|_2 < tol_1, \tag{13}$$

where $v_{k+1}^{(n+1)}$ and $v_k^{(n+1)}$ stand for the potential term obtained from two adjacent iterations, and tol_1 is an user-defined tolerance.

Once the decision criterion is satisfied, the time-evolution problem will propagate forward with one time step. Then the iterative process will be implemented on the same finite element space again for the new time step. The evolution will propagate forward all the time until the wavefunction converge or the following criterion is achieved

$$\sum \|\psi^{(n+1)} - \psi^{(n)}\|_2 < \mathrm{tol}_2, \tag{14}$$

where tol_2 is another user-defined tolerance.

Consider that the wavefunction varies much greater in the vicinity of the nuclei and between atoms of chemical bonds than in other regions, a mesh that contains a dense distribution of girds at these places while a sparse one in other places would be favoured to a uniform mesh with the same amount of grids. Based on this consideration, a mesh redistribution process is adopted. Detailed algorithm will be showed in the next section.

3. Mesh redistribution

In this section, we briefly review the mesh redistribution strategy introduced in [16,17], and discuss the generation of the monitor function in detail. To review the harmonic map based strategy, we first give Algorithm 1 for the flowchart of the algorithm, then the main components of the algorithm are introduced in the following subsections.

Algorithm 1 Mesh Redistribution based on harmonic maps

Require: The wavefunction $\psi^{(n)}$ at time $t^{(n)}$ and a regular fixed logical domain Ω_C with grid distribution $\mathcal{T}_{\text{ini}}$.

1: Obtain the mesh distribution $\mathcal{T}_C$ on Ω_C by solving the generated minimization problem by $\psi^{(n)}$.
2: **while** $\|\mathcal{T}_C - \mathcal{T}_{\text{ini}}\|_{L_\infty} > tol$ **do**
3: Use the difference between $\mathcal{T}_C$ and $\mathcal{T}_{\text{ini}}$ to achieve the movement of mesh grids on physical domain Ω.
4: Update the solution $\psi^{(n)}$ on the new mesh.
5: Solve the generated minimization problem by the updated $\psi^{(n)}$ to get $\mathcal{T}_C$.
6: **end while**

3.1. Mesh-redistribution algorithm based on harmonic maps

Consider two n-dimensional compact domain Ω and Ω_c with certain local coordinates $\overrightarrow{x}$ and $\overrightarrow{\xi}$, respectively. Denote a map $\overrightarrow{\xi} = \overrightarrow{\xi}(\overrightarrow{x})$ between Ω and Ω_c, then following Dvinsky and Brackbill the energy of this map can be written as

$$E(\overrightarrow{\xi}) = \frac{1}{2}\int_\Omega G^{ij}\frac{\partial \xi^\alpha}{\partial x^i}\frac{\partial \xi^\beta}{\partial x^j}\,\mathrm{d}\boldsymbol{x}, \tag{15}$$

where the inverse of G^{ij} is the monitor function and note that in this paper the Einstein summation convention is assumed. Following Li *et al.* [16], we call Ω the physical domain, Ω_c the logical domain, and $M = (G^{ij})^{-1}$ the monitor function.

To redistribute the mesh grids in a uniform manner, Li *et al.* [17] proposed a way to obtain the harmonic map from solving an optimization problem. For simplicity, we consider the physical problems in two space dimensions. Assume that Ω is a polyhedron. Let Γ_i and $\Gamma_{c,i}$ be the edges of Ω and Ω_c respectively. To maintain the geometrical characters of the physical domain with the movement of the boundary grids, a mapping which maps the vertexes (edges) of the physical domain to the corresponding vertexes (edges) of the logical domain should be adopted. Therefore, it's reasonable to consider the following mapping set from $\partial\Omega$ to $\partial\Omega_c$,

$$\begin{aligned}\boldsymbol{K} = \{\overrightarrow{\xi}_b \in C^0(\partial\Omega)|\,\overrightarrow{\xi}_b : \partial\Omega \to \partial\Omega_c;\ \overrightarrow{\xi}_b|_{\Gamma_i} \text{ is a piecewisely linear mapping without}\\ \text{degeneration of the Jacobian.}\}\end{aligned} \tag{16}$$

Existence and uniqueness are provided by the theory of Eells and Sampson [9] that for every $\overrightarrow{\xi}_b \in K$ there exists a unique $\overrightarrow{\xi} : \Omega \to \Omega_c$ such that $\overrightarrow{\xi}|_{\partial\Omega} = \overrightarrow{\xi}_b$ and $\overrightarrow{\xi}$ is the extreme of the functional (15). Based on the above discussion, we are going to solve the following problem

$$\begin{aligned}&\min \int_\Omega G^{ij}\frac{\partial \xi^k}{\partial x^i}\frac{\partial \xi^k}{\partial x^j}\,\mathrm{d}\boldsymbol{x},\\ &\text{s.t.}\ \overrightarrow{\xi}|_{\partial\Omega} = \overrightarrow{\xi}_b \in \boldsymbol{K}.\end{aligned} \tag{17}$$

Once the harmonic map $\overrightarrow{\xi}$ has been achieved, the difference between the new mesh given by $\overrightarrow{\xi}$ and the initial mesh on logical domain Ω_C is computed and will be used to redistribute the interior and boundary grids on the physical domain Ω.

Details of the Algorithm 1 are discussed in the following. Consider a two-dimensional physical domain Ω, assume that the mesh on Ω is denoted by $\mathcal{T}$ with $\mathcal{T}_i$ as its element, and $\mathcal{X}_i$ as its node. For the logical domain Ω_C, we use $\mathcal{T}_C$ to denote the associated mesh with $\mathcal{T}_{i,C}$ as its element, $\mathcal{A}_i$ as its node, respectively.

By solving the following optimization problem the initial mesh $\mathcal{T}_{\text{ini}}$ on Ω_C is generated

$$\begin{aligned} &\min \sum_k \int_\Omega \sum_i \left(\frac{\partial \xi^k}{\partial x^i}\right)^2 \mathrm{d}\boldsymbol{x} \\ &\text{s.t. } \overrightarrow{\xi}\,|_{\partial\Omega} = \overrightarrow{\xi}_b \in K. \end{aligned} \tag{18}$$

$\mathcal{T}_{\text{ini}}$ is only used as a reference and is fixed once obtained. In practice, if the physical domain is convex and is of regular shape (say a convex polygon), then we simply choose the physical domain as the logical domain with uniform initial mesh.

From Algorithm 1 the motion of the mesh on Ω is implemented in an iteration manner. Firstly we have to solve the optimization problem (17). Note that the efficiency of the solver for (17) is more important than its accuracy since by the solver we only try to improve the mesh property, that is, not the physical solution. However, the linear system generated from (17) is neither Hermitian nor positive definite, which results in difficulty for the efficient solver. To resolve the difficulty, it was suggested in [17] that the system be decoupled into two smaller systems: one is for the grid points on the boundary, and the other is for the interior grid points. Although there is also no good property for the first system, it is much smaller than the original system, and a generalized minimal residual method can be applied to solve it. For the second one, a multi-grid method is adopted to solve it because it is Hermitian and positive definite. Furthermore, Di *et al.* [7] proposed a new approach based on an algebraic multi-grid method to speed up the implementation for Equation (17). In our simulation this technique is adopted for solving Equation (17). We refer to Di *et al.* [7] and references therein for details.

Once $\overrightarrow{\xi}$ is obtained by solving Equation (17), the difference between the new mesh generated $\mathcal{T}_C$ from $\overrightarrow{\xi}$ and the fixed mesh $\mathcal{T}_{\text{ini}}$ on Ω_C will be computed. If L_∞ norm of the difference is small enough, that is,

$$\|\mathcal{T}_C - \mathcal{T}_{\text{ini}}\|_{L_\infty} < \text{tol}_3,$$

the iteration is then stopped, otherwise we will use the following procedures to get the movement of mesh grids on physical domain Ω.

If the L_∞ norm of the difference is greater than tol_3, the following formula is then used to generate the direction and magnitude of movement for each grid point on Ω,

$$\delta\mathcal{X}_i = \frac{\sum_{\mathcal{T}} |\mathcal{T}| \frac{\partial \boldsymbol{x}}{\partial \boldsymbol{\xi}}|_{\text{in } \mathcal{T}} \delta\mathcal{A}_i}{\sum_{\mathcal{T}} |\mathcal{T}|}, \tag{19}$$

where $\delta\mathcal{A}_i = \mathcal{A}_i^{\text{ini}} - \mathcal{A}_i$, and $\mathcal{T}$ stands for the element in the physical domain which has $\mathcal{X}_i$ as one of the vertexes, and $|\mathcal{T}|$ is its volume. $\partial\boldsymbol{x}/\partial\boldsymbol{\xi}$ is given by solving the following system in each element,

$$\begin{pmatrix} \dfrac{\partial x^1}{\partial \xi^1} & \dfrac{\partial x^1}{\partial \xi^2} \\ \dfrac{\partial x^2}{\partial \xi^1} & \dfrac{\partial x^2}{\partial \xi^2} \end{pmatrix} \begin{pmatrix} \mathcal{A}^1_{\mathcal{T}_c,1} - \mathcal{A}^1_{\mathcal{T}_c,0} & \mathcal{A}^1_{\mathcal{T}_c,2} - \mathcal{A}^1_{\mathcal{T}_c,0} \\ \mathcal{A}^2_{\mathcal{T}_c,1} - \mathcal{A}^2_{\mathcal{T}_c,0} & \mathcal{A}^2_{\mathcal{T}_c,2} - \mathcal{A}^2_{\mathcal{T}_c,0} \end{pmatrix} = \begin{pmatrix} \mathcal{X}^1_{\mathcal{T},1} - \mathcal{X}^1_{\mathcal{T},0} & \mathcal{X}^2_{\mathcal{T},1} - \mathcal{X}^2_{\mathcal{T},0} \\ \mathcal{X}^1_{\mathcal{T},2} - \mathcal{X}^1_{\mathcal{T},0} & \mathcal{X}^2_{\mathcal{T},2} - \mathcal{X}^2_{\mathcal{T},0} \end{pmatrix}, \tag{20}$$

where $(\mathcal{X}^1_{\mathcal{T},i}, \mathcal{X}^2_{\mathcal{T},i})$ represents the ith vertex of the element $\mathcal{T}$ in the physical domain Ω, and $(\mathcal{A}^1_{\mathcal{T}_c,i}, \mathcal{A}^2_{\mathcal{T}_c,i})$ represents the ith vertex of its corresponding element $\mathcal{T}_c$ in the logical domain Ω_c, here $i = 0, 1, 2$ in 2D case. It can be shown the above volume weighted average (19) converges to a smooth solution in measure when the size of the mesh goes to 0.

After we get $\delta\mathcal{X}_i$, the grid points in the physical domain Ω is updated by

$$\mathcal{X}_i^{\text{new}} = \mathcal{X}_i + \tau\delta\mathcal{X}_i, \tag{21}$$

where τ is a parameter in $[0, 1]$ and is used to avoid the mesh tangling.

The method for updating the wavefunction is one kind of interpolation-free solution-updating methods, which makes the implementation much simpler than the interpolation methods, and the details of the method is shown in the next subsection in this part.

Note that the monitor function in Equation (17) plays an important role in the simulations. A good monitor function can help on resolving the important regions in the physical domain with a smooth and regular enough mesh grid distribution. In the end of this part the design of the monitor function will be discussed.

3.2. Solution update

After the mesh-redistribution in the physical domain, we need to update the solution u on the new mesh. Each element $\mathcal{T}$ with its nodes $\mathcal{X}$ in the previous mesh corresponds uniquely to an element $\mathcal{T}^*$ with its nodes $\mathcal{X} + \tau\delta\mathcal{X}$ in the redistributed mesh. Also there is an affine map between the two elements. The combination of the affine maps from every element in the previous mesh to the corresponded element in the new mesh hence composes an piecewise affine map between the previous mesh and the new mesh. The surface of u on Ω will not change though the nodes of the mesh will be moved to new locations. Therefore, once we moved the mesh, an additional convection procedure that makes u 'flowing back' is necessary to keep u unchanged. Denote that the function of mesh movement $(\boldsymbol{\delta x})^k = (\delta\mathcal{X}_i)^k\Phi_i(\boldsymbol{x}, \tau)$ and $k = 1,2$ in two-dimensional case with $\Phi_i(\boldsymbol{x}, \tau)$ the basis function of the finite element space associated with the node $\mathcal{X}_i + \tau\delta\mathcal{X}_i$. Then the convection procedure can be governed by the following equation

$$u_\tau - \boldsymbol{\delta x} \cdot \nabla u = 0. \tag{22}$$

In the finite element space, u also can be expressed as

$$u = U_i(\tau)\Phi_i(\boldsymbol{x}, \tau), \tag{23}$$

where $U_i(\tau)$ is the value of u at the node $\mathcal{X}_i + \tau\delta\mathcal{X}_i$. Then the semi-discrete system for updating u can be deduced from the above result

$$\int_\Omega \left\{ \frac{\partial U_i(\tau)}{\partial \tau}\Phi_i(\boldsymbol{x}, \tau) - U_i(\tau)\frac{\partial \Phi_i}{\partial x^k}(\boldsymbol{\delta x})^k \right\} v \, \mathrm{d}\boldsymbol{x} = 0 \quad \forall v \in V_T(\Omega). \tag{24}$$

Let v be the basis functions of the finite element space, that is, $v = \Phi_j(\boldsymbol{x}, \tau)$, then a system of linear ODEs for U_i is obtained

$$\int_\Omega \Phi_i\Phi_j \, \mathrm{d}\boldsymbol{x}\frac{\partial U_i}{\partial \tau} = \int_\Omega \frac{\partial \Phi_i}{\partial x^k}(\boldsymbol{\delta x})^k\Phi_j \, \mathrm{d}\boldsymbol{x}U_i(\tau). \tag{25}$$

With a three-stage Runge–Kutta scheme the system can be solved. This procedure, based on the fact that the surface of u is not changed, provides an interpolation-free solution-updating in the new mesh.

3.3. Monitor function

From the expression of the optimization problem (17), the property of the moved mesh is determined by the monitor function. Therefore, the choose of the monitor function plays a very important role in the process of mesh redistribution. For different physical problems, different monitor functions are designed to obtain a desired mesh which can appropriately distribute the grids on the physical domain according to the problems. Generally, a mesh which has dense grid distribution in the regions where the solution varies heavily, that is, where the gradient of the solution is large, and sparse grid distribution on the places where the solution changes little is favoured. As for our model, because of

the existence of singularities a mesh with dense grid distribution around singularities is required. We choose the monitor function as below

$$M = \left(\sqrt{\epsilon + \sum_{i}^{\text{occ}} |\nabla \phi(\boldsymbol{x})|^2} \right) I, \tag{26}$$

where I stands for the identity matrix. With this monitor function the grid points move towards to the region around the singularity with large gradient of the wavefunctions, however, we also observe that in the region with small gradient far away from the singularity the grid points are almost kept unchanged, see the left of Figure 1. The new monitor function was then proposed to overcome the distortion,

$$M = \left(\sqrt{\epsilon + \tilde{n} + \sum_{i}^{\text{occ}} |\nabla \phi(\boldsymbol{x})|^2} \right) I, \tag{27}$$

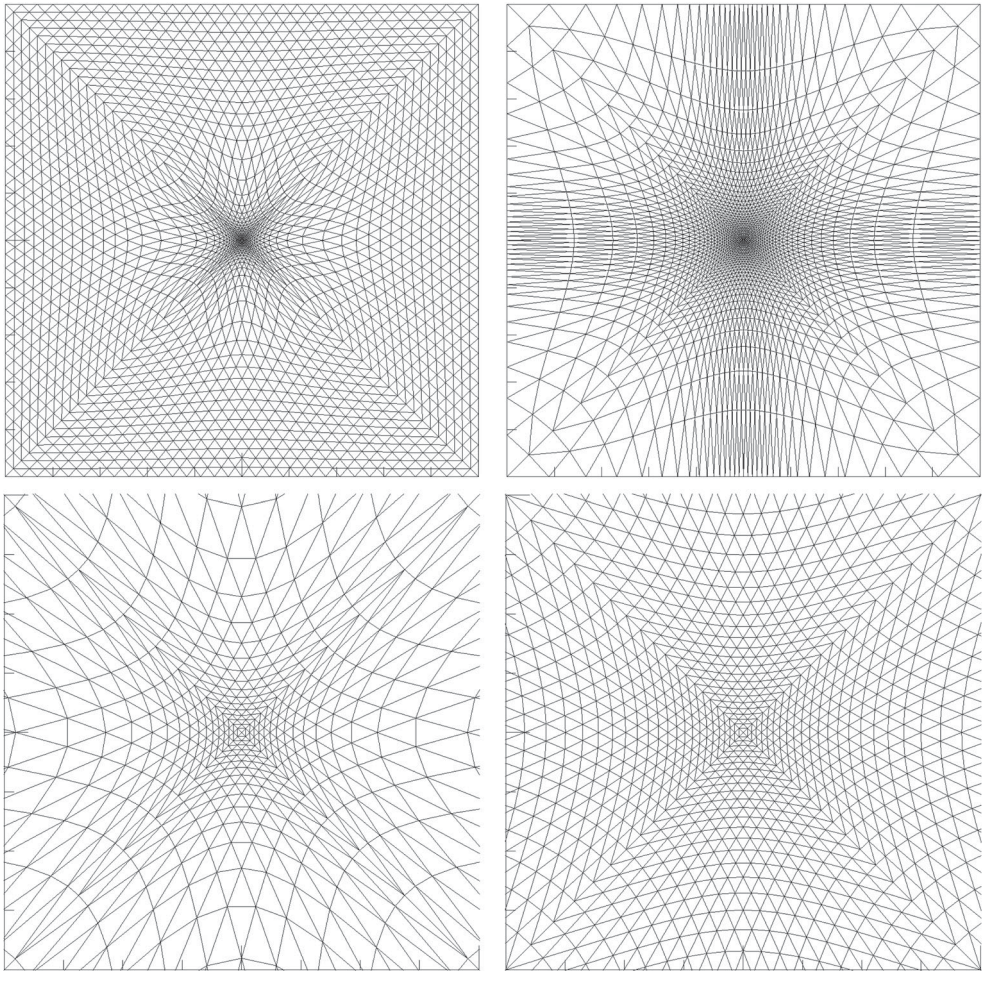

Figure 1. The top two figures show the meshes for the hydrogen system in the computational domain $[-10, 10]\times[-10,10]$ using monitor function $M_1 = (\sqrt{\epsilon + |\nabla\psi(\boldsymbol{r})|^2}\,)I$ (top left) and $M_2 = (\sqrt{\epsilon + |\nabla\psi(\boldsymbol{r})|^2 + \tilde{n}}\,)I$ (top right), respectively. The bottom two figures show the corresponding detailed meshes on domain $[-2, 2]\times[-2,2]$ around the nucleus.

where the new term $\tilde{n}$ is the solution of the following equation

$$\frac{\partial \tilde{n}}{\partial t} - \delta \Delta \tilde{n} = 0 \tag{28}$$

with the initial condition $\tilde{n}^0 = \sum_i^{occ} |\nabla \phi_i(\boldsymbol{x})|^2$ and δ a parameter depends on the size of the physical domain. With the diffuse term $\tilde{n}$ in the monitor function, the grid redistribution process gives a mesh with better regularity and smoothness which sufficiently improves the mesh quality, see the right of Figure 1.

Based on the Harmonic maps, we can get a mesh which obtains the properties mentioned in the last section from the initial uniform mesh. The mesh redistribution process happens between two adjacent imaginary time step which results in that the mesh redistribution process is relatively independent on the time evolution problem. Precisely, the movement of the mesh based on Harmonic maps takes place after obtaining a numerical solution from the partial differential equation (PDE) solver at time $t^{(n)}$. Once the mesh is determined, the finite element space will be rebuilt and the numerical solution will be updated. Then the PDE solver will be adopted in the new mesh to obtain the numerical solution at time $t^{(n+1)}$ and the mesh redistribution process will be applied again. In this way, we can separate the algorithm for solving the problem (4) into two parts, one is numerically solving the PDE discussed above and the other is mesh redistribution. The PDE solver pass the mesh and numerical solution to mesh redistribution solver, and the mesh redistribution solver returns the new mesh and updated numerical solution back to the PDE solver. The algorithm is showed in Algorithm 2.

Algorithm 2 Solving Schrödinger equation

Require: A random initial wavefunction $\psi^{(0)}$ satisfying the boundary condition, start time $t^{(0)} = 0$, and time step Δt.

while $\|\psi^{(n+1)} - \psi^{(n)}\|_{L_2} > tol_1$ **do**
  $t^{(n+1)} = t^{(n)} + \Delta t$;
  Implement Algorithm 1.
  $k = 0$;
  while $\|\psi_{k+1}^{(n+1)} - \psi_k^{(n+1)}\|_{L_2} > tol_2$ **do**
    if $k = 0$ **then** $\psi_k^{(n+1)} = \psi^n$
    end if
    Solve the system to obtain $\psi_{k+1}^{(n+1)}$ using the numerical method presented above.
  end while
end while

4. Numerical examples

In this section, the effectiveness of the proposed method is tested by three examples. In the first example, the ground state of a hydrogen atom is simulated, and the advantage of the moving mesh method can be observed obviously. Besides the ground state of a given system, the excited states can also be simulated with the proposed method, which is shown by our second example in which an anharmonic oscillator system is considered. In the last example, a coupled Gross–Pitaevskii system is examined numerically, and the results successfully show that the proposed method can also be used to handle the nonlinear problem.

4.1. Two-dimensional hydrogen atom

In two-dimensional case, the stationary Schrödinger equation of the hydrogen atom is written as

$$-\frac{1}{2}\nabla^2 u - \frac{1}{|x|}u = \lambda u. \tag{29}$$

The lowest eigenvalue of this equation is -2.0. For the derivation, please refer to the appendix. The physical domain for this problem is designed as $[-10, 10] \times [-10, 10]$. The uniform meshes are generated from refining the coarsest mess which contains 145 points. As discussed in Section 2.1, as long as the initial state does not orthogonal to the ground state of the system, the wavefunction will converge to the ground state. Thus generally, a random guess can be used as the initial condition. The wavefunction is propagated from time $\tau = 0$ to $\tau = 100$ with imaginary time step $\Delta\tau = 0.2$ in this experiment. The results are showed in the left of Figure 2. From the figure we can see that with the redistribution of the mesh both the convergence rate and accuracy achieved are superior to that of a fixed mesh. The convergence rate of the solver with mesh redistribution reaches 2.0, which shows that the eigenvalue problem converges at an expected rate of convergence for the linear finite element method. Besides the numerical accuracy, the CPU time needed in the simulation is also studied. The results are shown in the right of Figure 2. From the results, we can see that to get the same accuracy of the numerical solution, our mesh redistribution method always needs less mesh grids and CPU time compared to the fixed mesh case.

4.2. Anharmonic oscillator

This example concerns a non-separable non-degenerate two-dimensional anharmonic oscillator system [6] which is designed to test the algorithm proposed in this paper. The Hamiltonian is given by

$$\begin{aligned} H &= -\nabla^2 + V(x, y) \\ &= -\frac{\partial^2}{\partial x^2} - \frac{\partial^2}{\partial y^2} + (4xy^2 + 2x + 1)^2 \\ &\quad + (4x^2 y + 2\sqrt{2}y + \sqrt{2})^2 - 4(x^2 + y^2) - (2 + 2\sqrt{2}). \end{aligned}$$

The computational domain is chosen as $[-4, 4] \times [-4, 4]$ on which an initial uniform mesh containing 333 grid points is set. To check the convergence of the presented algorithm, four other initial

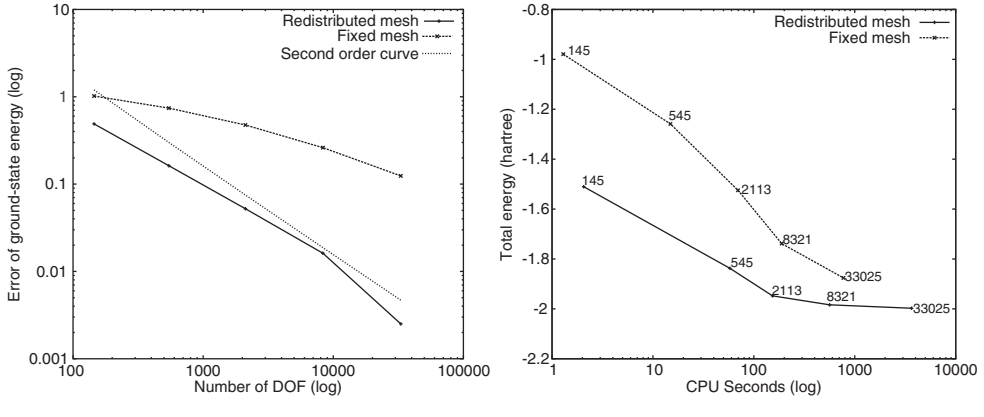

Figure 2. Left: Convergence rate of the eigenvalue with fixed uniform mesh and with moving mesh for the two-dimensional hydrogen system. The exact ground-state value is -2. Right: CPU time needed for the simulations. The number in the figure stands for the number of mesh grids in each simulation.

meshes are obtained by successively refining the coarsest initial mesh. To achieve the ground state, first and second excited states, three random orthogonal wavefunctions are propagated simultaneously from time $\tau = 0$ to $\tau = 2.5$ with the imaginary time step $\Delta\tau = 0.001$. The exact ground state energy for the anharmonic oscillator is $E_0 = 0$. For the excited states we compare the result with a Chebyshev polynomial discrete variable representation (DVR) calculation using 3600 basis functions [6,18]. The DVR results of the first and second excited states are $E_1 = 4.36598$ and $E_2 = 7.0667$, respectively. The numerical results using our method are demonstrated in Table 1, which are in agreement with DVR results and shows that the convergence rate is in accord with the analysis of the method we employed.

Table 1. Numerical errors and convergence order for the two-dimensional oscillator system: Error_0, Error_1 and Error_2 represent the error of energies of the ground state, first and second excited states, respectively.

DOF	Error_0	rate_0	Error_1	rate_1	Error_2	rate_2
333	4.44996×10^{-1}	–	1.38691×10^{0}	–	1.40222×10^{0}	–
1265	1.16386×10^{-1}	1.94	3.83720×10^{-1}	1.85	3.70973×10^{-1}	1.92
4929	2.94208×10^{-2}	1.98	9.74203×10^{-2}	1.98	9.42285×10^{-2}	1.98
19457	7.37918×10^{-3}	2.00	2.44961×10^{-2}	1.99	2.37104×10^{-2}	1.99
77313	1.84640×10^{-3}	2.00	6.13481×10^{-3}	2.00	5.98698×10^{-3}	1.99

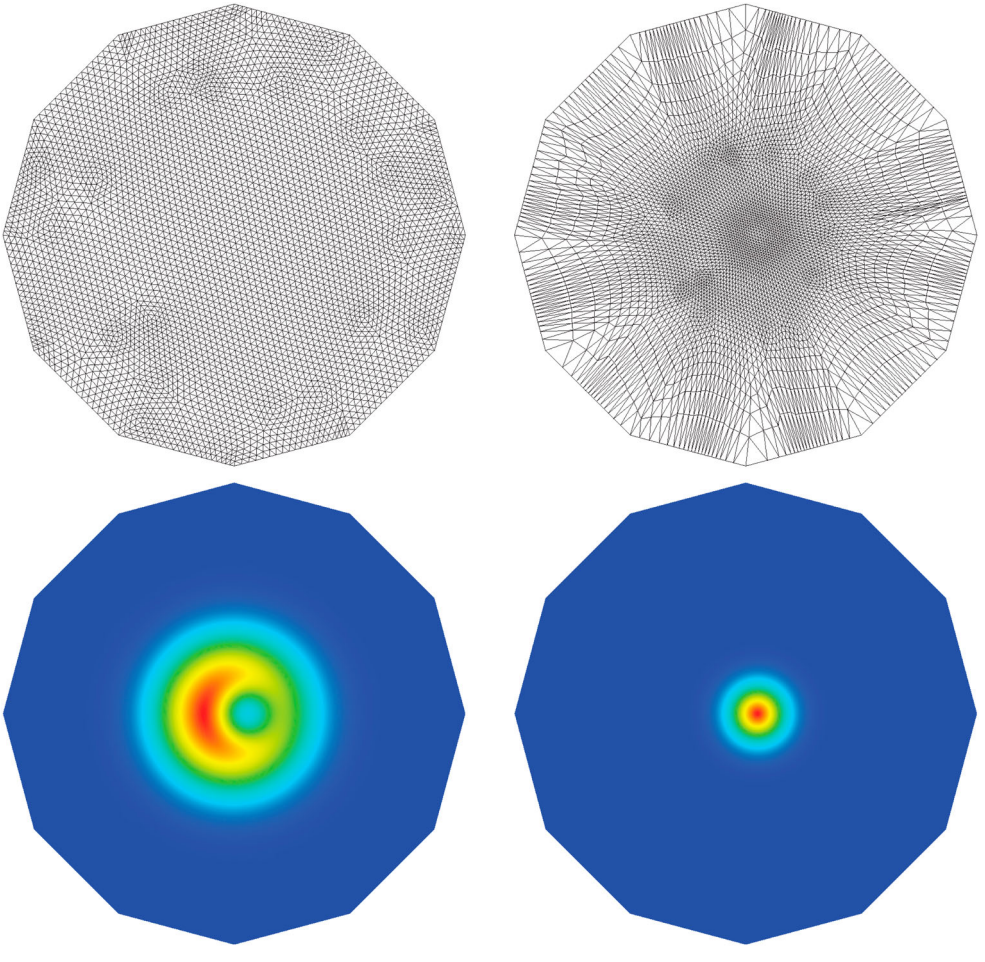

Figure 3. The ground state for the coupled Gross–Pitaevskii system. Top left: the initial uniform mesh with 8321 mesh grids. Top right: the redistributed mesh. Bottom: the ground state of the GPES where the left is for $\psi^{(1)}$ and the right is for $\psi^{(2)}$.

4.3. A coupled Gross–Pitaevskii system

In this example we take a two-dimensional condensate [3] into account. We use our method to compute the ground state of the coupled Gross–Pitaevskii equations. This experiment well demonstrate the reliability of our method and nicely illustrate the effect of phase segregation. The system consist of two GPEs,

$$\begin{aligned} \mathrm{i}\partial_t \psi^{(l)} &= \left[-\frac{1}{2}\nabla^2 + U_l + \sum_{k=1}^{2} v_{lk} |\psi^{(k)}|^2 \right] \psi^{(l)} \\ \|\psi^{(l)}\|_{L^2}^2 &= N_l, \quad l = 1, 2 \end{aligned} \tag{30}$$

with scaled and off-centred harmonic potentials (see, e.g. [1])

$$U_l = \tfrac{1}{2}[(\omega_{1l}(x - x_l))^2 + (\omega_{2l}(y - y_l))^2]$$

with

$$\omega_{11} = \omega_{21} = \pi, x_1 = y_1 = 0, \omega_{12} = \omega_{22} = 3\pi, x_2 = 0.19, y_2 = 0$$

and the intra-species coupling constants

$$v_{11} = 1.3 \times 10^{-6}, \quad v_{12} = v_{21} = 1.0 \times 10^{-6}, \quad v_{22} = 1.3 \times 10^{-11}.$$

We set the same number of the particles $N_1 = N_2 = 10^7$. Then we perform our numerical experiments with different monitor functions on domain $[-3, 3] \times [-3, 3]$ with 4305 grid points. From the results of Figure 3 we can see the phase segregation clearly which agrees with the observation in [3].

5. Conclusions

In this paper, an adaptive finite element algorithm using ITP is proposed to solve the two-dimensional Schrödinger equation. The numerical discretization consists of the Crank–Nicolson scheme for the tempoal discretization, and the linear finite element method for the spatial discretization. To handle the singularity appeared in the simulations, a moving mesh method is proposed to redistribute the mesh grids, and the design of the monitor function is discussed in detail. A prediction–correction procedure is introduced to resolve the nonlinearity of the problem. Numerical experiments successfully show that desired convergence order can be obtained from the simulations on the successively refined meshes, and that quality mesh is generated during the simulations with the moving mesh module in the algorithm which improves the numerical solution effectively.

One future work is to explore the applications of the proposed numerical method in this paper for solving more complex systems in Kohn–Sham density functional theory, which potentially is a competitive alternative for the calculations of the ground state of the electronic structures, compared with solving the nonlinear eigenvalue problems.

Disclosure statement

No potential conflict of interest was reported by the authors.

Funding

The first author would like to thank the support from Postgraduate Studentship from University of Macau. The work of the second author is partially supported by Fundo para o Desenvolvimento das Ciências e da Tecnologia (FDCT)

029/2016/A1, 050/2014/A1 from Macao SAR, MYRG2017-00189-FST, MYRG2014-00109-FST from University of Macau, and National Natural Science Foundation of China [Grant No. 11401608].

References

[1] W. Bao, *Ground states and dynamics of multicomponent Bose–Einstein condensates*, Multiscale Model. Simul. 2(2) (2004), pp. 210–236.
[2] G. Bao, G. Hu, and D. Liu, *Numerical solution of the Kohn–Sham equation by finite element methods with an adaptive mesh redistribution technique*, J. Sci. Comput. 55(2) (2013), pp. 372–391.
[3] M. Caliari, A. Ostermann, S. Rainer, and M. Thalhammer, *A minimisation approach for computing the ground state of Gross–Pitaevskii systems*, J. Comput. Phys. 228(2) (2009), pp. 349–360.
[4] S.A. Chin, S. Janecek, and E. Krotscheck, *Any order imaginary time propagation method for solving the Schrödinger equation*, Chem. Phys. Lett. 470(4) (2009), pp. 342–346.
[5] M.L. Chiofalo, S. Succi, and M.P. Tosi, *Ground state of trapped interacting Bose–Einstein condensates by an explicit imaginary-time algorithm*, Phys. Rev. E 62(5) (2000), pp. 7438.7444
[6] C-C. Chou and D.J. Kouri, *Multidimensional supersymmetric quantum mechanics: A scalar Hamiltonian approach to excited states by the imaginary time propagation method*, J. Phys. Chem. A 117(16) (2013), pp. 3449–3457.
[7] Y. Di, R. Li, and T. Tang, *A general moving mesh framework in 3D and its application for simulating the mixture of multi-phase flows*, Commun. Comput. Phys. 3(3) (2008), pp. 582–602.
[8] A.S. Dvinsky, *Adaptive grid generation from harmonic maps on Riemannian manifolds*, J. Comput. Phys. 95(2) (1991), pp. 450–476.
[9] J. Eells and J.H. Sampson, *Harmonic mappings of Riemannian manifolds*, Amer. J. Math. 86(1) (1964), pp. 109–160.
[10] J.-L. Fattebert and M.B. Nardelli, *Finite difference methods for ab initio electronic structure and quantum transport calculations of nanostructures*, Handb. Numer. Anal. 10 (2003), pp. 571–612.
[11] C. Fiolhais, F. Nogueira, and M.A.L. Marques, *A Primer in Density Functional Theory*, Vol. 620, Springer-Verlag, Berlin, 2003.
[12] J. Geiser, *Fourth-order splitting methods for time-dependant differential equations*, Numer. Math. Theor. Methods Appl. 1(3) (2008), pp. 321–339.
[13] E.P. Gross, *Structure of a quantized vortex in boson systems*, Il Nuovo Cimento Series 10 20(3) (1961), pp. 454–477.
[14] G. Kresse and J. Furthmüller, *Efficient iterative schemes for ab initio total-energy calculations using a plane-wave basis set*, Phys. Rev. B 54(16) (1996), p. 11169.
[15] L. Lehtovaara, J. Toivanen, and J. Eloranta, *Solution of time-independent Schrödinger equation by the imaginary time propagation method*, J. Comput. Phys. 221(1) (2007), pp. 148–157.
[16] R. Li, T. Tang, and P. Zhang, *Moving mesh methods in multiple dimensions based on harmonic maps*, J. Comput. Phys. 170(2) (2001), pp. 562–588.
[17] R. Li, T. Tang, and P. Zhang, *A moving mesh finite element algorithm for singular problems in two and three space dimensions*, J. Comput. Phys. 177(2) (2002), pp. 365–393.
[18] J.C. Light, I.P. Hamilton, and J.V. Lill, *Generalized discrete variable approximation in quantum mechanics*, J. Chem. Phys. 82(3) (1985), pp. 1400–1409.
[19] L. Lin, J. Lu, L. Ying, and E. Weinan, *Adaptive local basis set for Kohn–Sham density functional theory in a discontinuous Galerkin framework I: Total energy calculation*, J. Comput. Phys. 231(4) (2012), pp. 2140–2154.
[20] K. Majava, R. Glowinski, and T. Kärkkäinen, *Solving a non-smooth eigenvalue problem using operator-splitting methods*, Int. J. Comput. Math. 84(6) (2007), pp. 825–846.
[21] R.I. McLachlan, G. Reinout, and W. Quispel, *Splitting methods*, Acta Numer. 11 (2002), pp. 341–434.
[22] J.E. Pask and P.A. Sterne, *Finite element methods in ab initio electronic structure calculations*, Model. Simul. Mater. Sci. Eng. 13(3) (2005), pp. R71–R96
[23] L.P. Pitaevskii, *Vortex lines in an imperfect bose gas*, Sov. Phys. JETP 13(2) (1961), pp. 451–454.
[24] B. Satarić, V. Slavnić, A. Belić, A. Balaž, P. Muruganandam, and S.K. Adhikari, *Hybrid OpenMP/MPI programs for solving the time-dependent Gross–Pitaevskii equation in a fully anisotropic trap*, Comput. Phys. Commun. 200 (2016), pp. 411–417.
[25] G. Strang, *On the construction and comparison of difference schemes*, SIAM. J. Numer. Anal. 5(3) (1968), pp. 506–517.
[26] P. Suryanarayana, V. Gavini, T. Blesgen, K. Bhattacharya, and M. Ortiz, *Non-periodic finite-element formulation of Kohn–Sham density functional theory*, J. Mech. Phys. Solids 58(2) (2010), pp. 256–280.
[27] T. Torsti, T. Eirola, J. Enkovaara, T. Hakala, P. Havu, V. Havu, T. Höynälänmaa, J. Ignatius, M. Lyly, I. Makkonen, T.T. Rantala, J. Ruokolainen, K. Ruotsalainen, E. Räsänen, H. Saarikoski, and M.J. Puska, *Three real-space discretization techniques in electronic structure calculations*, Physica Status Solidi (b) 243(5) (2006), pp. 1016–1053.
[28] L.E. Young-S, D. Vudragović, P. Muruganandam, S.K. Adhikari, and A. Balaž, *OpenMP Fortran and C programs for solving the time-dependent gross–Pitaevskii equation in an anisotropic trap*, Comput. Phys. Commun. 204 (2016), pp. 209–213.

Appendix. Ground state energy to a hydrogen atom in two-dimensional space

Here analytic method for obtaining the ground state energy of two-dimensional hydrogen system is shown. The system can be described by the following equation

$$\left[-\frac{1}{2}\nabla^2 - \frac{1}{|\boldsymbol{r}|}\right]\psi(\boldsymbol{r}) = E\psi(\boldsymbol{r})$$

with the nucleus located at the origin. Using polar coordinates $\boldsymbol{r} = (r, \theta)$ and then we separate the wavefunction

$$\psi(\boldsymbol{r}) = R(r)Y(\theta).$$

With the Laplacian expression in polar coordinates

$$\nabla^2 = \frac{\partial^2}{\partial r^2} + \frac{1}{r}\frac{\partial}{\partial r} + \frac{1}{r^2}\frac{\partial^2}{\partial \theta^2}$$

the Schrödinger equation then becomes

$$\frac{r^2}{R}\left(\frac{d^2R}{\mathrm{d}r^2} + \frac{1}{r}\frac{\mathrm{d}R}{\mathrm{d}r}\right) + 2r^2\left(\frac{1}{r} + E\right) = -\frac{1}{Y}\frac{d^2Y}{\mathrm{d}\theta^2},$$

which follows that

$$\frac{1}{Y}\frac{d^2Y}{\mathrm{d}\theta^2} = -m^2;$$

$$\frac{1}{2}\left(\frac{d^2R}{\mathrm{d}r^2} + \frac{1}{r}\frac{\mathrm{d}R}{\mathrm{d}r}\right)$$

$$-\frac{m^2}{2r^2}R + \left(\frac{1}{r} + E\right)R = 0.$$

Now set $\kappa = \sqrt{-2E}$, $\rho = \kappa r$ and $\rho_0 = 2/\kappa$. Then

$$\left(\frac{d^2R}{\mathrm{d}\rho^2} + \frac{1}{\rho}\frac{\mathrm{d}R}{\mathrm{d}\rho}\right) - \frac{m^2}{\rho^2}R + \left(\frac{\rho_0}{\rho} - 1\right)R = 0.$$

Since the spectrum is symmetric under $m \to -m$, we can choose $m \geq 0$. After looking at the $\rho \to 0$ and $\rho \to \infty$ behaviour of $R(\rho)$, $R(\rho)$ must have the form like $\rho^m\,\mathrm{e}^{-\rho}v(\rho)$, as a result $v(\rho)$ should satisfy

$$\rho v''(\rho) + (2m + 1 - 2\rho)v' - (2m + 1 - \rho_0)v = 0.$$

Now expand $v(\rho)$ to a power series $v(\rho) = \sum_0^\infty c_j\rho^j$. Substitute $v(\rho)$ in the above differential equation and rearrange the terms then we obtain the following relationship

$$c_{j+1} = \frac{2j + 2m + 1 - \rho_0}{j(j+1) + (j+1)(2m+1)}c_j.$$

Let us assume that the series contain an infinite number of terms. For large j, the coefficients of the series behave like

$$\frac{c_{j+1}}{c_j} \to \frac{2}{j}, \text{ that is: } c_j \sim \frac{2^j}{j!}.$$

Recall that $\mathrm{e}^\rho = \sum_j \rho^j/j!$, whose coefficient is even less than $\frac{2^j}{j!}$, we see that the recursion relation between c_j produces a function $v(r)$ that grows faster than e^ρ, that is, produces non-physical diverging solutions. To prevent this from happening, the power series of v should be terminated, which gives

$$\rho_0 = 2j_{\max} + 2|m| + 1 \quad \text{for } j_{\max} \geq 0,$$

where we have used the $m \to -m$ symmetry to replace m by $|m|$. Finally we get

$$\rho_0 = 2k + 1 \quad \text{with } k = 0, 1, 2\ldots;$$

$$\kappa = \frac{2}{\rho_0} = \frac{2}{2k+1};$$

$$E = -\frac{1}{2}\kappa^2 = -\frac{1}{2}\frac{1}{(k + 1/2)^2}.$$

Hence the ground state energy of 2D hydrogen atom should be $E_0 = -2$.